

# PCCP

Accepted Manuscript



This is an *Accepted Manuscript*, which has been through the Royal Society of Chemistry peer review process and has been accepted for publication.

*Accepted Manuscripts* are published online shortly after acceptance, before technical editing, formatting and proof reading. Using this free service, authors can make their results available to the community, in citable form, before we publish the edited article. We will replace this *Accepted Manuscript* with the edited and formatted *Advance Article* as soon as it is available.

You can find more information about *Accepted Manuscripts* in the [Information for Authors](#).

Please note that technical editing may introduce minor changes to the text and/or graphics, which may alter content. The journal's standard [Terms & Conditions](#) and the [Ethical guidelines](#) still apply. In no event shall the Royal Society of Chemistry be held responsible for any errors or omissions in this *Accepted Manuscript* or any consequences arising from the use of any information it contains.

## Thermodynamics of $\text{Fe}_3\text{O}_4$ - $\text{Co}_3\text{O}_4$ and $\text{Fe}_3\text{O}_4$ - $\text{Mn}_3\text{O}_4$ Spinel Solid Solutions at Bulk and Nanoscale

Sulata K. Sahu<sup>1</sup>, Baiyu Huang<sup>2</sup>, Kristina Lilova<sup>1</sup>, Brian F. Woodfield<sup>2</sup> Alexandra Navrotsky<sup>1\*</sup>

<sup>1</sup>*Peter A. Rock Thermochemistry Laboratory and NEAT ORU, University of California Davis,*

*Davis, CA 95616, USA*

<sup>2</sup>*Department of Chemistry and Biochemistry, Brigham Young University,*

*Provo, UT 84602, USA*

\*Corresponding author, e-mail: [anavrotsky@ucdavis.edu](mailto:anavrotsky@ucdavis.edu)

### Abstract

High temperature oxide melt solution calorimetry has been performed to investigate the enthalpies of mixing ( $\Delta_{\text{mix}}H$ ) of bulk and nanophase  $(1-x)\text{Fe}_3\text{O}_4 - x\text{M}_3\text{O}_4$  ( $M = \text{Co}, \text{Mn}$ ) spinel solid solutions. The entropies of mixing ( $\Delta_{\text{mix}}S$ ) were calculated from the configurational entropies based on cation distributions and the Gibbs free energies of mixing ( $\Delta_{\text{mix}}G$ ) were obtained. The  $\Delta_{\text{mix}}H$  and  $\Delta_{\text{mix}}G$  for  $(1-x)\text{Fe}_3\text{O}_4 - x\text{Co}_3\text{O}_4$  system is negative over the complete solid solution range, for both macroscopic and nanoparticulate materials. In  $(1-x)\text{Fe}_3\text{O}_4 - x\text{Mn}_3\text{O}_4$ , the formation enthalpies from cubic  $\text{Fe}_3\text{O}_4$  (magnetite) and tetragonal  $\text{Mn}_3\text{O}_4$  (hausmannite) are negative for  $\text{Mn}_3\text{O}_4$  mole fractions less than 0.67 and slightly positive for higher manganese content. Relative to cubic  $\text{Fe}_3\text{O}_4$  and cubic  $\text{Mn}_3\text{O}_4$  (stable at high temperature) the enthalpies and Gibbs energies of mixing are negative over the entire composition range. A combination of measured mixing enthalpies and reported Gibbs energies in the literature provides experimental entropies of mixing. The experimental entropies of mixings are consistent with those calculated from cation distributions for  $x > 0.3$ , but the experimental values are

smaller than those predicted for  $x < 0.3$ . This discrepancy may be related to the calculations having treated  $\text{Fe}^{2+}$  and  $\text{Fe}^{3+}$  as distinguishable species. The measured surface energies of the  $(1-x)\text{Fe}_3\text{O}_4 - x\text{M}_3\text{O}_4$  solid solutions are in the range 0.6 - 0.9 J/m<sup>2</sup>, similar to those of many other spinels. Because the surface energies are relatively constant, the thermodynamics of mixing at a given particle size throughout the solid solution can be considered independent of the particular particle size, thus confirming and extending the conclusions of a recent study on iron spinels.

**Keywords:** Normal and Inverse Spinels,  $\text{Fe}_3\text{O}_4 - \text{Co}_3\text{O}_4$  and  $\text{Fe}_3\text{O}_4 - \text{Mn}_3\text{O}_4$  Solid solutions, Calorimetry, Thermodynamics, Enthalpies of mixing, Cation distribution, Configurational entropy, Gibbs energies of mixing.

## Introduction

Spinels of iron, cobalt and manganese ( $\text{Co}_3\text{O}_4$ ,  $\text{Fe}_3\text{O}_4$ ,  $\text{Mn}_3\text{O}_4$ ) and their solid solutions are the subject of extensive research because of their applications in electrochemistry, catalysis, fuel cells, water splitting and other fields <sup>1, 2</sup>.  $\text{Fe}_3\text{O}_4$  has an inverse spinel structure  $\text{Fe}^{3+}[\text{Fe}^{2+}\text{Fe}^{3+}]\text{O}_4$ , with one  $\text{Fe}^{3+}$  per formula unit on tetrahedral sites and the remaining  $\text{Fe}^{2+}$  and  $\text{Fe}^{3+}$  are randomly distributed on octahedral sites <sup>3</sup>.  $\text{Mn}_3\text{O}_4$  and  $\text{Co}_3\text{O}_4$  are normal spinels,  $\text{M}^{2+}[\text{M}^{3+}\text{M}^{3+}]\text{O}_4$  with  $\text{M}^{2+}$  in tetrahedral sites and  $\text{M}^{3+}$  in octahedral sites and their extent of disorder is expected to remain small at higher temperatures due to the large octahedral site preference of  $\text{M}^{3+}$  <sup>4, 5</sup>.  $\text{Mn}_3\text{O}_4$  is tetragonal at ambient conditions but transforms at a cubic structure at  $\sim 1170$  °C <sup>6</sup>.

As the applications of these spinels depend on their temperature range of stability and thermodynamic properties, numerous thermodynamic studies have been carried out on them, mostly at macroscopic level, with emphasis on free energies of formation and mixing <sup>7-20</sup>. The thermodynamic properties of bulk binary oxide solid solutions ( $\text{Mn}_3\text{O}_4 - \text{Fe}_3\text{O}_4$ ,  $\text{Co}_3\text{O}_4 - \text{Fe}_3\text{O}_4$ ,

Mn<sub>3</sub>O<sub>4</sub> - Co<sub>3</sub>O<sub>4</sub>) have been studied extensively, mainly by phase equilibrium and modeling methods<sup>11, 21, 22</sup>. The activity - composition relations in ternary solid solutions have been determined using electrochemical measurements and attempts were made to obtain enthalpies and entropies of mixing from the temperature dependence of EMF and other studies<sup>23, 24</sup>. Aukrust and Muan measured the activity-composition relations in Co<sub>3</sub>O<sub>4</sub> - Fe<sub>3</sub>O<sub>4</sub> and Mn<sub>3</sub>O<sub>4</sub> - Co<sub>3</sub>O<sub>4</sub> by studying the equilibrium phase relations between these and binary rocksalt oxides CoO - "FeO" and MnO - CoO<sup>25-27</sup>. Oxidation - reduction enthalpies of the Co<sub>3</sub>O<sub>4</sub>-Fe<sub>3</sub>O<sub>4</sub> system were determined at 900-1200 °C from equilibrium oxygen pressure measurements of the ferrites Co<sub>x</sub>Fe<sub>2-x</sub>O<sub>4</sub> in equilibrium with a coexisting rocksalt phase by Schmalzried and Tretjakow<sup>28</sup>, whereas Jonker<sup>29</sup> determined them from electrical measurements near room temperature. Diffusion coefficients of Co and Fe in CoFe<sub>2</sub>O<sub>4</sub> were used to study the Co<sub>3</sub>O<sub>4</sub> - Fe<sub>3</sub>O<sub>4</sub> system by Muller and Schmalzried<sup>30</sup>. Thermodynamics of mixing of bulk Fe<sub>3</sub>O<sub>4</sub> - Co<sub>3</sub>O<sub>4</sub>, Fe<sub>3</sub>O<sub>4</sub> - Mn<sub>3</sub>O<sub>4</sub> and Mn<sub>3</sub>O<sub>4</sub> - Co<sub>3</sub>O<sub>4</sub> spinel solid solutions were calculated by Navrotsky<sup>21</sup> based on an oxidation - reduction and cation distribution approach. This work stressed the importance of internal oxidation - reduction equilibria, which provide significant negative enthalpy terms and of the cation redistribution which strongly favors the location of trivalent cobalt and manganese on octahedral sites. The values of enthalpy, entropy, and free energy of mixing calculated by Navrotsky are comparable to Muan's experimental values<sup>25</sup>. The more recent experimental determination of the mixing enthalpies of Fe<sub>3</sub>O<sub>4</sub> - Mn<sub>3</sub>O<sub>4</sub> solid solution by high temperature oxide melt solution calorimetry by Guillemet-Fritsch et al<sup>31</sup> are in a reasonable agreement with the earlier calculated mixing properties<sup>11, 21</sup>.

Despite these earlier studies, separating the effects of enthalpy and entropy on the Gibbs energy of mixing in these complex solid solutions is difficult without independent calorimetric

measurements of the enthalpy of mixing, which has only been done for the bulk  $\text{Mn}_3\text{O}_4 - \text{Fe}_3\text{O}_4$  system. Furthermore the thermodynamics of mixing of nanoscale solid solutions in these systems have not been studied, although the surface energies of  $\text{Mn}_3\text{O}_4$  and  $\text{Fe}_3\text{O}_4$  have been determined<sup>32</sup>. Hence the present work is a systematic study of the mixing properties of  $\text{Fe}_3\text{O}_4 - \text{Co}_3\text{O}_4$  and  $\text{Fe}_3\text{O}_4 - \text{Mn}_3\text{O}_4$  spinel solid solutions at bulk and nano scales using high temperature oxide melt solution calorimetry. Combining experimentally determined enthalpies of mixing with previously measured free energies of mixing enables calculation of entropies of mixing. These experimental enthalpies and entropies are compared with those calculated independently of the present calorimetric data by applying the O'Neill-Navrotsky model of spinel cation distribution energetics<sup>33</sup>. The obtained surface energies are compared to those from earlier studies for other spinels<sup>32</sup>.

Previous investigations suggest a number of spinel phases have lower surface energy than other oxides of the same metal<sup>32</sup> and it seems probable that this behavior can be extended to the transition metal spinel solid solutions. To investigate this, we prepared nanophase as well as bulk solid solutions and determined their surface energies from the differences in drop solution enthalpies of bulk and nano spinel solid solutions as a function of their BET surface areas. The goal of the present investigation is to obtain a systematic picture of mixing properties in Fe, Co, Mn spinels at macroscopic and nano scales.

## Experimental Methods

### *Synthesis*

Nanocrystallite solid solutions  $(1-x)\text{Fe}_3\text{O}_4 - x\text{Co}_3\text{O}_4$  with compositions  $\text{Co}_{0.6}\text{Fe}_{2.4}\text{O}_4$ ,  $\text{CoFe}_2\text{O}_4$ ,  $\text{Co}_{1.5}\text{Fe}_{1.5}\text{O}_4$ ,  $\text{Co}_2\text{FeO}_4$ , and  $\text{Co}_{2.4}\text{Fe}_{0.6}\text{O}_4$  and  $(1-x)\text{Fe}_3\text{O}_4 - x\text{Mn}_3\text{O}_4$  with compositions  $\text{MnFe}_2\text{O}_4$ ,  $\text{Mn}_{1.5}\text{Fe}_{1.5}\text{O}_4$ ,  $\text{Mn}_2\text{FeO}_4$ ,  $\text{Mn}_{2.4}\text{Fe}_{0.6}\text{O}_4$  were synthesized via chemical co-precipitation

methods.<sup>34-36</sup> Briefly, stoichiometric amounts of  $\text{Co}(\text{NO}_3)_2 \cdot 6\text{H}_2\text{O}$  /  $\text{MnCl}_2 \cdot 4\text{H}_2\text{O}$  and  $\text{Fe}(\text{NO}_3)_3 \cdot 9\text{H}_2\text{O}$  salts were dissolved in distilled water to prepare a stock solution of pH 0.5. The stock solution was stirred for 10 min to yield a transparent aqueous solution. The precipitating agent NaOH solution with pH 13.7 was added drop-wise while stirring the stock solution to achieve final pH 12. The solution was heated at 100–110 °C with magnetic stirring for 2 h, followed by heating at 140 - 150 °C for 1 h. The black colored gel was washed with distilled water several times and then dried at 110 °C overnight and then calcined at 250 °C for 2 h. Pure nanocrystalline  $\text{Co}_3\text{O}_4$  and  $\text{Mn}_3\text{O}_4$  were prepared by a solvent deficient method developed by Woodfield et al.<sup>37</sup> All the bulk phase samples were prepared by calcining the corresponding nanocrystalline phase in a vacuum furnace at elevated temperatures for 24 h.

### ***Characterization***

Powder X-ray diffraction (XRD) patterns were collected using a Bruker AXS D8 Advance diffractometer ( $\text{CuK}\alpha$  radiation). Data were recorded from 10° to 70° ( $2\theta$ ) at a step size of 0.02 ° ( $2\theta$ ) and a collection time of 2 s/step. Phase identification and crystallite sizes were determined using Jade 6.1 software and the PDF file version 2.0 (Materials Data Inc., Livermore, CA).

The surface areas of the synthesized nanocrystalline spinels were determined by  $\text{N}_2$  adsorption using the Brunauer–Emmett–Teller (BET) method at -196 °C<sup>38</sup>. Ten-point nitrogen adsorption isotherms were collected in a relative pressure range of  $p/p^0 = 0.05\text{--}0.3$  (where,  $p^0$  = saturation pressure) using a Micromeritics ASAP 2020 surface area and porosity analyzer. Prior to analysis, the samples were degassed under vacuum at 300 °C for 4 h. The uncertainties in the BET surface area measurements were propagated from fitting a straight line to  $1/[Q(p^0/p_1)]$  ( $Q =$

quantity adsorbed, mmol/g) vs  $p/p^0$  using the Micromeritics software. The total amount of water on the nanocrystalline samples were determined by thermo gravimetric analysis using a Setaram LabSys Evo. The sample was heated in a platinum crucible from 25 °C to 700 °C in an oxygen atmosphere at 10 °C/min. A buoyancy correction was made by subtracting the baseline collected by running an identical experiment with an empty platinum crucible. The water content was determined from the TGA weight loss curve.

### ***High temperature oxide melt solution calorimetry***

The drop solution enthalpies were measured in a custom-made isoperibol Tian - Calvet twin microcalorimeter described previously<sup>39-41</sup>. Pellets of approximately 5 mg were loosely pressed, weighed, and dropped from room temperature into molten  $3\text{Na}_2\text{O}\cdot 4\text{MoO}_3$  solvent at 700 °C. Measurements were repeated 8 – 10 times for each sample to achieve statistically reliable data. The calorimeter was calibrated using the heat content of 5 mg pellets of high purity  $\alpha\text{-Al}_2\text{O}_3$  (99.997%, Alfa Aesar), dropped into an empty Pt crucible. Before the drop solution experiments, all samples were equilibrated at 25 °C and  $50 \pm 5$  % humidity in the calorimetry suite, and the water contents of these equilibrated samples were determined using TGA as described in the previous section. Surface energy calculations from high temperature drop solution calorimetry data were completed as described in earlier studies<sup>41</sup>.

## **Results and Discussion**

### ***Structural characterization***

The X-ray powder diffraction data confirm single-phase spinels without impurities. The crystallite size of the nano  $(1-x)\text{Fe}_3\text{O}_4 - x\text{M}_3\text{O}_4$  solid solution determined from XRD is shown in Table 1. The BET surface areas ( $A$ ) of the nano  $\text{Fe}_3\text{O}_4 - \text{Co}_3\text{O}_4$  and  $\text{Fe}_3\text{O}_4 - \text{Mn}_3\text{O}_4$  solid solutions

range from 9300 to 22900 m<sup>2</sup>/mol (Table 1). The particle sizes calculated from BET surface area are similar to the XRD crystallite sizes calculated using the Scherrer equation<sup>42</sup> applied to the line broadening of diffraction peaks indicating that there is no significant agglomeration in the synthesized nanoparticles.

### ***Surface enthalpy from calorimetric data***

The measured average drop solution enthalpies ( $\Delta_{ds}H$ ) of Co<sub>3</sub>O<sub>4</sub>, Mn<sub>3</sub>O<sub>4</sub> and the solid solutions are given in Table 1. To determine the surface enthalpies of the solid solutions,  $\Delta_{ds}H$  of Fe<sub>3</sub>O<sub>4</sub> and  $\Delta_{ds}H$  of bulk (1-x)Fe<sub>3</sub>O<sub>4</sub> - xMn<sub>3</sub>O<sub>4</sub> solid solution in molten 3Na<sub>2</sub>O·4MoO<sub>3</sub> at 700°C has been taken from Lilova et al.<sup>43</sup> and Guillemet-Fritsch et al.<sup>31</sup>, whereas the  $\Delta_{ds}H$  of Co<sub>3</sub>O<sub>4</sub>, Mn<sub>3</sub>O<sub>4</sub> and the bulk and nano (1-x)Fe<sub>3</sub>O<sub>4</sub> - xCo<sub>3</sub>O<sub>4</sub> and nano (1-x)Fe<sub>3</sub>O<sub>4</sub> - xMn<sub>3</sub>O<sub>4</sub> solid solution series has been determined in the present study. The surface enthalpies (referring to hydrated surfaces) were determined from the drop solution enthalpies as described in our previous work<sup>41, 44</sup>. The difference between the enthalpy of drop solutions,  $\Delta_{ds}H$ , of the bulk and nano samples, corrected for water content, arises from the surface enthalpy term ( $\gamma \times A$ , where  $A$  is the surface area and  $\gamma$  is the surface enthalpy, essentially equivalent to the surface energy and, as argued previously, very similar to the surface free energy<sup>32</sup>). The surface enthalpy is given by:

$$\gamma = [\Delta_{ds}H (\text{bulk}) - \Delta_{ds}H (\text{nano})] / A \quad (1)$$

Since all nanocrystalline samples contain adsorbed water on their surfaces, the  $\Delta_{ds}H$  values were corrected for water content following procedures described previously<sup>45-48</sup>. The thermochemical cycle used for water correction is given in Table 2 and the determined surface enthalpies are presented in Table 1. The calculated surface enthalpies for hydrated surfaces of both solid solutions range between 0.6 and 0.9 J/m<sup>2</sup>. These results are consistent with the general trends observed that spinels have low surface energies (0.5 to 1 J/m<sup>2</sup>)<sup>32, 49</sup>.

### *Enthalpies of mixing from calorimetric data*

$\Delta_{ds}H$  of both bulk and nano solid solutions display a significant deviation from linear behavior (see Figures 1 and 2). The drop solution enthalpies (after correcting for water in the nano sample) can be fitted into a third degree polynomial;  $y = A + B_1x + B_2x^2 + B_3x^3$ . The enthalpies of mixing ( $\Delta_{mix}H$ ) of the spinel solid solutions were determined from the differences in the measured  $\Delta_{ds}H$  of the solid solution and the weighted average of the mechanical mixture of the end-members. They can be represented by a subregular solution (Margules formalism),  $\Delta_{mix}H = x(1-x)[W_1(1-x) + W_2x]$  kJ/mol, where  $x$  is the mole fraction of  $M_3O_4$  and  $W_1$  and  $W_2$  are the excess mixing (interaction) parameters. The interaction parameters  $W_1$  and  $W_2$  relates to the coefficient of the polynomial expressions representing the drop solution enthalpy as  $W_1 = B_2 + B_3$  and  $W_2 = B_2 + 2B_3$ . The mixing enthalpies of bulk and nano  $(1-x)Fe_3O_4 - xM_3O_4$  solid solutions are shown in Figures 3 and 4. The  $\Delta_{mix}H$  for  $(1-x)Fe_3O_4 - xCo_3O_4$  system is negative over the complete solid solution range, both in macroscopic and nano scale. For  $(1-x)Fe_3O_4 - xMn_3O_4$  system, the mixing enthalpies from cubic  $Fe_3O_4$  (magnetite) and tetragonal  $Mn_3O_4$  (hausmannite) are negative for  $0 \leq x_{Mn_3O_4} \leq \sim 0.67$  and become slightly positive for  $\sim 0.67 \leq x_{Mn_3O_4} \leq 1$ . It is noted that the spinel solid solutions of  $(1-x)Fe_3O_4 - xMn_3O_4$  systems are cubic for  $0 \leq x_{Mn_3O_4} \leq 0.6$  and tetragonal for  $0.6 \leq x_{Mn_3O_4} \leq 1$ .

Because of this difference in structure, the enthalpies of mixing described above are better called enthalpies of formation, and the change in structure means that, strictly speaking, a polynomial representation of this enthalpy is not strictly correct. Although the tetragonal – cubic transition in  $Mn_3O_4$  appears first order<sup>6</sup>, there does not appear to be a well defined two phase region for coexistence of cubic and tetragonal spinel in the solid solutions, rather the tetragonality appears to diminish gradually<sup>31</sup>. Thus at intermediate compositions, the transition may be higher order and a single curve representing enthalpy of mixing may be appropriate.

The effect of enthalpy of the tetragonal to cubic transition of  $\text{Mn}_3\text{O}_4$ ,  $\Delta_{t-c}H$  on the enthalpies of mixing has been discussed by Guillemet-Fritsch et al.<sup>31</sup>. They suggest that the influence of  $\Delta_{t-c}H$  of  $\text{Mn}_3\text{O}_4$  on energetics of the solid solutions appears to be small at  $0.5 < x_{\text{Mn}_3\text{O}_4} < 0.8$ , i.e. in the vicinity of the change in symmetry. The tetragonality ( $c/a$  ratio) of the solid solutions diminishes rapidly with decreasing  $\text{Mn}_3\text{O}_4$  content and the  $\Delta_{t-c}H$  diminishes rapidly from its value of  $20.8 \text{ kJ mol}^{-1}$  at  $x = 1$  to a very small or zero value near  $x = 0.6$ . Based on these arguments, the enthalpies of mixing of  $(1-x)\text{Fe}_3\text{O}_4 - x\text{Mn}_3\text{O}_4$  spinel solid solution relative to  $c\text{-Mn}_3\text{O}_4$  and  $c\text{-Fe}_3\text{O}_4$  were determined by taking into account of  $\Delta_{t-c}H$   $\text{Mn}_3\text{O}_4$  and Table 3 presents the detailed thermochemical cycle. Relative to  $c\text{-Mn}_3\text{O}_4$  and  $c\text{-Fe}_3\text{O}_4$  the enthalpies of mixing are negative all over the composition range.

The intermediate compositions in the  $(1-x)\text{Fe}_3\text{O}_4 - x\text{M}_3\text{O}_4$  spinel solid solutions gradually change from the inverse spinel structure ( $\text{Fe}_3\text{O}_4$ ) to the normal structure ( $\text{Co}_3\text{O}_4$  and  $\text{Mn}_3\text{O}_4$ )<sup>21,31</sup>. It has been suggested that the ordering effect of the cation redistribution (change from partially to completely inverse) would produce a small negative heat of mixing whereas the lattice strain arising from the small size mismatch would result in a small positive heat of mixing.<sup>33, 50, 51</sup> Moreover the electron exchange reaction ( $\text{Fe}^{2+} + \text{M}^{3+} = \text{Fe}^{3+} + \text{M}^{2+}$ ) in both magnetite - containing systems results in significant negative heat of mixing<sup>21</sup>. Furthermore, the change in the structure from cubic to tetragonal symmetry system contributes to the heat of mixing, as discussed above. Hence, the obtained mixing enthalpies of the two spinel solid solutions are result of the combined effect of the above competing factors. Below we try to separate these factors and provide a quantitative description of the mixing thermodynamics.

### *Enthalpies of mixing from O'Neill and Navrotsky model*

Our approach is to calculate the enthalpy of mixing of solid solutions using O'Neill and Navrotsky thermodynamic model<sup>33</sup>. According to the model, the total enthalpy of mixing ( $\Delta_{\text{mix}}H$ ) is the sum of mixing enthalpies due to (A) electron exchange ( $\Delta_{\text{mix,e,e}}H$ ), (B) cation distributions ( $\Delta_{\text{mix,c,d}}H$ ) in tetrahedral and octahedral sites and (C) size mismatch ( $\Delta_{\text{s.m.}}H$ ) factor,

$$\Delta_{\text{mix}}H = \Delta_{\text{mix,e,e}}H + \Delta_{\text{mix,c,d}}H + \Delta_{\text{s.m.}}H \quad (2)$$

The details of calculation of the individual mixing enthalpies are described as follow

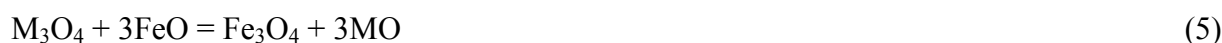
#### *Enthalpies of mixing due to electron exchange reactions ( $\Delta_{\text{mix,e,e}}H$ )*

The enthalpy of mixing due to electron exchange is given in equation (3);

$$\Delta_{\text{mix,e,e}}H = \Delta_{\text{ox/red,ss}}H - \Delta_{\text{ox/red,mm}}H \quad (3)$$

$$\text{where, } \Delta_{\text{ox/red,mm}}H = x(\Delta_{\text{ox/red}}H, \text{M}_3\text{O}_4) + (1-x)(\Delta_{\text{ox/red}}H, \text{Fe}_3\text{O}_4) \quad (4)$$

Oxidation–reduction enthalpies of the solid solutions ( $\Delta_{\text{ox/red,ss}}H$ ), due to the electron exchange reaction between different cations on octahedral sites ( $\text{M}^{3+}_{\text{B}} + \text{Fe}^{2+}_{\text{B}} = \text{M}^{2+}_{\text{B}} + \text{Fe}^{3+}_{\text{B}}$ ) were calculated based on the Navrotsky model (spinel-rocksalt reactions)<sup>21</sup> as the difference in reaction enthalpies of equation (5) and (6)



where  $\text{M}^{2+}_{\text{A}}$ ,  $\text{Fe}^{3+}_{\text{B}}$ ,  $\text{M}^{2+}_{\text{B}}$ ,  $\text{Fe}^{3+}_{\text{A}}$  are the individual cations occupying tetrahedral (A) and octahedral sites (B). The enthalpies of eq. 5 ( $\Delta H_5$ ) and 6 ( $\Delta H_6$ ) represent the difference in the formation enthalpies and site preference enthalpies of the products and reactants, respectively.

The calculated  $\Delta_{\text{ox/red,ss}}H$  at 25 °C are,

For  $(1-x)\text{Fe}_3\text{O}_4 - x\text{Co}_3\text{O}_4$

$$\Delta_{\text{ox/red,ss}}H = 0.5(\Delta H_9 - \Delta H_{10}) = -52.96 \text{ kJ/mol, where } \Delta H_9 = -108.00 \text{ kJ/mol } \Delta H_{10} = -2.09 \text{ kJ/mol}$$

For  $(1-x)\text{Fe}_3\text{O}_4 - x\text{Mn}_3\text{O}_4$

$$\Delta_{\text{ox/red,ss}}H = 0.5\Delta H_9 = -36.67 \text{ kJ/mol, where } \Delta H_9 = -73.33 \text{ kJ/mol and } \Delta H_{10} = 0 \text{ kJ/mol.}$$

The obtained  $\Delta_{\text{mix,e,e}}H$  based on above calculations are exothermic and vary between -47.3 and -6.5 kJ/mol for  $(1-x)\text{Fe}_3\text{O}_4 - x\text{Co}_3\text{O}_4$  solid solutions. For  $(1-x)\text{Fe}_3\text{O}_4 - x\text{Mn}_3\text{O}_4$ , the obtained  $\Delta_{\text{mix,e,e}}H$  with cubic  $\text{Fe}_3\text{O}_4$  and tetragonal  $\text{Mn}_3\text{O}_4$  end members are between -38.2 and -5.6 kJ/mol. For both systems,  $\Delta_{\text{mix,e,e}}H$  is found to be minimum at  $x = 0.33$ , where maximum number of cations take part in the oxidation - reduction reactions (Table 4).

#### *Enthalpies of mixing due to cation distributions ( $\Delta_{\text{mix,c,d}}H$ )*

The O'Neill and Navrotsky thermodynamic model was used to determine the cation distribution enthalpies in  $(1-x)\text{Fe}_3\text{O}_4 - x\text{M}_3\text{O}_4$  spinel solid solutions<sup>33</sup>. The model was formulated by minimizing the free energy of disorder, in which disordering enthalpy varies linearly with the inversion parameter and the disordering entropy is related to configurational entropy ( $S_{\text{conf}}$ ). Based on literature data,  $\text{Mn}^{3+}$  and  $\text{Co}^{3+}$  have strong octahedral preference and occupies exclusively the octahedral site whereas  $\text{M}^{2+}$ ,  $\text{Fe}^{2+}$ , and  $\text{Fe}^{3+}$  are randomly distributed on both tetrahedral and octahedral sites<sup>6, 52</sup>. In the present calculation,  $\text{Fe}^{2+}$  and  $\text{Fe}^{3+}$  are assumed to be distinguishable species. The cation distributions in the tetrahedral and octahedral sites of individual compositions are shown in Table 5. Based on the cation distributions and on the assumption, the disordering enthalpy ( $\Delta_{\text{dis,ss}}H$ ) of the solid solutions takes the following form<sup>33</sup>, the  $\Delta_{\text{dis,ss}}H$  is given by equation 7.

$$\Delta_{\text{dis,ss}}H = a [\alpha_{\text{Fe}^{2+}-\text{Fe}^{3+}} + \beta (a+b)] + b [\alpha_{\text{M}^{2+}-\text{Fe}^{3+}} + \beta (a+b)] \quad (7)$$

where  $a$  and  $b$  are the mole fractions of  $\text{Fe}^{3+}$  and  $\text{M}^{2+}$ , the wrong cations present in tetrahedral and octahedral sites respectively.  $\alpha$  and  $\beta$  are the interchange enthalpy parameters. The values of

$\alpha$  and  $\beta$  are expected to be comparable in magnitude but opposite in sign. It was found that for 2-3 spinels,  $\beta$  term takes values between -15 and -25 kJ/mol and an average value of -20 kJ/mol can be adopted<sup>33, 51</sup>. In the present work,  $\alpha_{M2+-Fe3+}$  and  $\alpha_{Fe2+-Fe3+}$  were calculated from the differences in the cation site preference enthalpies<sup>33, 51</sup>.

The enthalpies of mixing arising from the cation redistribution ( $\Delta_{\text{mix,c,d}}H$ ) were calculated as the difference between the disordering enthalpy of mechanical mixtures ( $\Delta_{\text{dis,mm}}H$ ) of the end-members ( $\text{Fe}_3\text{O}_4$  and  $\text{M}_3\text{O}_4$ ) and the solid solution ( $\Delta_{\text{dis,ss}}H$ ) by the following expression,

$$\Delta_{\text{mix,c,d}}H = \Delta_{\text{dis,ss}}H - \Delta_{\text{dis,mm}}H \quad (8)$$

$$\text{where, } \Delta_{\text{dis,mm}}H = (1-x)(\Delta_{\text{dis}}H \text{ Fe}_3\text{O}_4) + x (\Delta_{\text{dis}}H \text{ M}_3\text{O}_4) \quad (9)$$

The calculated values of  $\Delta_{\text{mix,c,d}}H$  for  $(1-x)\text{Fe}_3\text{O}_4 - x\text{M}_3\text{O}_4$  are exothermic and the maximum exothermicity was obtained at  $x = 0.67$ .  $\Delta_{\text{mix,c,d}}H$  for  $(1-x)\text{Fe}_3\text{O}_4 - x\text{Co}_3\text{O}_4$  solid solutions varies between -0.4 and -9.9 kJ/mol and for  $(1-x)\text{Fe}_3\text{O}_4 - x\text{Mn}_3\text{O}_4$ , it ranges between -0.2 and -7.6 kJ/mol (Table 4). Hence, the cation redistributions further stabilizes the solid solution in terms of enthalpy.

#### *Mixing enthalpy due to size mismatch ( $\Delta_{\text{mix, s,m}}H$ )*

The effect of the size mismatch were taken into account using the simplest possible regular solution model<sup>33</sup>. The enthalpy of mixing arising from the size mismatch source is given as

$$\Delta_{\text{mix, s,m}}H = Wx(1-x) \quad (10)$$

where  $W$  is  $(239.3 \Theta V + 0.3)$  kJ/mol<sup>32, 35</sup> and  $\Theta V$  is the volume mismatch term given by  $(V_2 - V_1) / [0.5(V_2 + V_1)]$ . The molar volumes of the solid solutions were calculated from the measured lattice parameters. The estimated enthalpies of mixing for  $(1-x)\text{Fe}_3\text{O}_4 - x\text{Co}_3\text{O}_4$  solid solutions, varies between 0.2 and 1.2 kJ/mol and for  $(1-x)\text{Fe}_3\text{O}_4 - x\text{Mn}_3\text{O}_4$  solid solutions with cubic  $\text{Fe}_3\text{O}_4$

and cubic  $\text{Mn}_3\text{O}_4$  end members, it ranges between 0.4 and 1.4 kJ/mol. The observed small endothermic  $\Delta_{\text{mix,s,m}}H$  indicates little contribution to the total mixing enthalpy. However, for  $(1-x)\text{Fe}_3\text{O}_4 - x\text{Mn}_3\text{O}_4$  solid solutions with cubic  $\text{Fe}_3\text{O}_4$  and tetragonal  $\text{Mn}_3\text{O}_4$  end members,  $\Delta_{\text{mix,s,m}}H$  are between 0.4 and 16.0 kJ/mol. For  $x < 0.6$ ,  $\Delta_{\text{mix,s,m}}H$  is close to zero, and for  $0.6 \leq x < 1$ ,  $\Delta_{\text{mix,s,m}}H$  increases to 16.0 kJ/mol (Table 4). This relatively large endothermic mixing of the spinel solid solutions for  $0.6 \leq x_{\text{Mn}_3\text{O}_4} < 1$  reflects the increase in tetragonality ( $c/a$  ratio) of the solid solutions with manganese content.

The calculated total mixing enthalpies, contributed by the above factors are shown in Figures 3 and 4(a). The enthalpies of mixing in the cubic solid solution, calculated by consideration of the tetragonal to cubic phase transition enthalpy are shown in Figure 4 (b). For both systems the major contribution to the mixing enthalpy arises from the electron exchange reactions and the mixing enthalpies have a minimum at  $x = 0.33$ , where the maximum number of ions take part in the oxidation - reduction reaction. The  $\Delta_{\text{mix}}H$  for  $(1-x)\text{Fe}_3\text{O}_4 - x\text{Co}_3\text{O}_4$  system, calculated using this model is negative over the complete solid solution range. In  $(1-x)\text{Fe}_3\text{O}_4 - x\text{Mn}_3\text{O}_4$ , the mixing enthalpies from cubic  $\text{Fe}_3\text{O}_4$  and tetragonal  $\text{Mn}_3\text{O}_4$  are negative for  $0 \leq x \leq \sim 0.6$  and becomes slightly positive for  $\sim 0.6 \leq x \leq 1$ . However the  $\Delta_{\text{mix}}H$  of  $(1-x)\text{Fe}_3\text{O}_4 - x\text{Mn}_3\text{O}_4$  solid solutions relative to cubic  $\text{Fe}_3\text{O}_4$  and cubic  $\text{Mn}_3\text{O}_4$  are negative over the entire composition range. The calculated mixing enthalpies using the O'Neill and Navrotsky thermodynamic model compares well with the experimentally determined  $\Delta_{\text{mix}}H$  for both the  $(1-x)\text{Fe}_3\text{O}_4 - x\text{Co}_3\text{O}_4$  and  $(1-x)\text{Fe}_3\text{O}_4 - x\text{Mn}_3\text{O}_4$  systems (see Fig. 3 and 4).

### Entropies and Gibbs free energies of mixing

For a spinel  $A_{1-y}B_x(A_yB_{2-y})O_4$  with inversion parameter  $y$ , the configurational entropy ( $S_{\text{conf}}$ ) can be written in the following form,

$$S_{\text{conf}} = -R \left\{ y \ln y + (1 - y) \ln(1 - y) + 2 \left[ \frac{y}{2} \ln \frac{y}{2} + \left(1 - \frac{y}{2}\right) \ln \left(1 - \frac{y}{2}\right) \right] \right\} \quad (11)$$

The configurational entropy starts from zero for a normal spinel, maximizes at 15.48 J/(mol K) for random cation distribution ( $y = 2/3$ ) and is  $2R \ln 2$  or 11.53 J/(mol K) for a totally inverse spinel<sup>53</sup>. In the present work, the configurational entropy,  $S_{\text{conf}}$  of each composition of  $(1-x)\text{Fe}_3\text{O}_4 - x\text{M}_3\text{O}_4$  spinel solid solution series has been calculated using the site occupancy data (Table 3), assuming  $\text{Fe}_3\text{O}_4$  as an inverse spinel,  $\text{Mn}_3\text{O}_4$  and  $\text{Co}_3\text{O}_4$  as normal, and intermediate spinels have maximum oxidation of  $\text{Fe}^{2+}$  to  $\text{Fe}^{3+}$  and a cation distribution in which  $\text{Mn}^{3+}$  and  $\text{Co}^{3+}$  are octahedral but all other cations are randomly distributed. Table 3 shows the configurational entropy and entropies of mixing) of  $(1-x)\text{Fe}_3\text{O}_4 - x\text{M}_3\text{O}_4$  solid solutions, where

$$\Delta_{\text{mix}}S = S_{\text{conf}}(\text{solid solutions}) - xS_{\text{conf}}(\text{Fe}_3\text{O}_4) - (1 - x)S_{\text{conf}}(\text{M}_3\text{O}_4) \quad (\text{M: Co, Mn}) \quad (12)$$

Figures 5(a) and (b) show the configurational entropies and the calculated entropies of mixing of the solid solution vs.  $x_{\text{M}_3\text{O}_4}$ .

Aukrust and Muan<sup>25</sup> experimentally determined the activity–composition relations of the  $\text{Fe}_3\text{O}_4\text{--Co}_3\text{O}_4$  solid solutions at 1200 °C. The electrochemical measurements of Tret'yakov<sup>17</sup> in the temperature range 900 - 1200 °C provided activity–composition relations in cubic  $\text{Fe}_3\text{O}_4\text{--Mn}_3\text{O}_4$  solid solutions. Tables 6 and 7 presents the calculated Gibbs free energies of mixing, ( $\Delta_{\text{mix}}G$ ) for  $(1-x)\text{Fe}_3\text{O}_4 - x\text{Co}_3\text{O}_4$  and  $(1-x)\text{Fe}_3\text{O}_4 - x\text{Mn}_3\text{O}_4$ , systems calculated from these data. The experimental entropies of mixing,  $\Delta_{\text{mix}}S$  can be calculated as  $\Delta_{\text{mix}}S = (\Delta_{\text{mix}}H - \Delta_{\text{mix}}G) / T$ ; where  $\Delta_{\text{mix}}H$  is the measured enthalpy of mixing which is approximated to be independent of

temperature. We pick  $T$  as the middle of the temperature range of the free energy measurements. The strict uncertainty associated with this experimental value of  $\Delta_{\text{mix}}S$  is hard to estimate, but it will be probably between  $\pm 5$  and  $\pm 8$  J/(mol K) and arises from uncertainties in the calorimetric data, approximate fit of the calorimetric data and the uncertainties of the activity data.

These experimental entropies of mixing can be compared with the entropies of mixing obtained from the configurational entropies calculated using the O'Neill and Navrotsky model. (shown in Table 4 and 5). The experimental entropies of mixing at  $x < 0.3$  appears to be small or close to zero. At  $x > 0.3$ , experimental  $\Delta_{\text{mix}}S$  scatters around the  $\Delta_{\text{mix}}S$  values calculated based on the configurational entropies. In  $(1-x)\text{Fe}_3\text{O}_4 - x\text{Mn}_3\text{O}_4$  system at  $x > 0.6$ , the experimental values are similar to but perhaps slightly more positive than those from the cation distribution model. There may be several reasons for these differences. (1) The entropy model may be inappropriate when both  $\text{Fe}^{2+}$  and  $\text{Fe}^{3+}$  are present because of rapid electron hopping between  $\text{Fe}^{2+}$  and  $\text{Fe}^{3+}$ , leading to local electronic entropy rather than a configurational term from positional disorder. The communal entropy arising from electron hopping between  $\text{Fe}^{2+}$  and  $\text{Fe}^{3+}$  may be destroyed in the solid solution by the addition of cobalt/manganese and the oxidation of  $\text{Fe}^{2+}$  to  $\text{Fe}^{3+}$ . This would occur at  $0 < x < 0.33$  (at  $x > 0.33$  little or no  $\text{Fe}^{2+}$  is present). Thus it is not clear how one should calculate the entropy of mixing in this regime. (2) There may be existence of systematic errors in the measured activities reported in the literature; such errors would be largest near the end members. (3) The solid solutions themselves may have more ordered cation distributions at lower  $x$ . However, very extensive ordering would be required to decrease the entropies substantially. (4) Differences in vibrational entropy terms may be significant, but these would need to provide a negative contribution to the entropy of mixing (lower vibrational entropy in the

solid solution than in a mixture of end members). Thus we suspect the electronic term is the dominant cause of the discrepancy at  $x < 0.33$ .

Gibbs energies of mixing of  $(1-x)\text{Fe}_3\text{O}_4 - x\text{M}_3\text{O}_4$ , systems were calculated from the measured mixing enthalpies by calorimetric techniques and entropies of mixing based on the configurational entropies and were compared with those obtained from the experimentally determined activity composition relations<sup>17, 25</sup>. The calculated  $\Delta_{\text{mix}}G$  from the present work generally agrees well with  $\Delta_{\text{mix}}G$  obtained from activity - composition relations (Figures 6(a-c)). The calculated  $\Delta_{\text{mix}}G$  displays large negative deviations from ideal Gibbs energies of mixing ( $\Delta_{\text{mix}}G^{\text{ld}}$ ) indicating the stabilization of the solid solutions over the mechanical mixture of the end members. This stabilization can be attributed to more energetically favorable redistribution of cations and valences in the solid solutions.

The enthalpies of mixing of  $(1-x)\text{Fe}_3\text{O}_4 - x\text{M}_3\text{O}_4$  spinel solid solutions in macroscopic and nano scales are similar within the error limits. Such similar mixing energetics of spinel solid solutions in macroscopic and nano scale suggests that the thermodynamics of mixing is independent of the particle size provided similar or nearly similar particle size is maintained throughout the solid solution and its end members. As the surface energies of the  $(1-x)\text{Fe}_3\text{O}_4 - x\text{M}_3\text{O}_4$  spinel solid solutions are relatively constant, the thermodynamics of mixing, at a given particle size throughout the solid solution, can be considered independent of the particular particle size. The observed result thus confirms and extends the conclusions of a recent study on iron spinels by Lilova et al<sup>49</sup>, where the energetics of macroscopic and nano sized  $\text{Fe}_3\text{O}_4 - \text{Fe}_2\text{TiO}_4$  spinel solid solutions were studied using high temperature oxide melt solution calorimetry.

Throughout this work we have assumed the cation distribution model can be applied to both bulk and nanoscale solid solutions, i.e. both have the same cation distribution for a given composition. Without any direct evidence for the cation distributions in the nanophase materials, no other approach is possible. Because the bulk spinels are quite disordered, any changes in the cation distribution at the nanoscale, perhaps toward more disorder, will affect the thermodynamics relatively little.

## Conclusions

Thermodynamic mixing of macroscopic and nano scale spinel solid solutions of  $(\text{Fe}_3\text{O}_4 - \text{M}_3\text{O}_4)$  (M: Co, Mn) systems have been investigated employing high temperature oxide melt solution calorimetry and using the O'Neill and Navrotsky thermodynamic model. The observed  $\Delta_{\text{mix}}H$  of  $(1-x)\text{Fe}_3\text{O}_4 - x\text{M}_3\text{O}_4$  spinel solid solutions at macroscopic and nano are independent of the particle size provided similar or nearly similar particle size is maintained throughout the solid solution and its end members. Assuming the site occupancies are similar for bulk and nano solid solutions, their entropies of mixing based on cation distribution will be the same and hence the Gibbs free energy of mixing curves will retain their shape regardless of the average particle size. The surface energies of the spinel solid solution series ranges between 0.6 and 0.9 J/m<sup>2</sup>, which confirms the previous observations that spinel phases have lower surface energy than other oxides of the same metal.

## Acknowledgements

S.K.S., K.L, and A.N. thank financial support for sample characterization, calorimetry, and data analysis and manuscript preparation by the U.S. Department of Energy, Office of Science, Office of Basic Energy Sciences, under Award DE-FG02-05ER15667. B.H. and B.F.W. were supported by US Department of Energy under Grant DE-FG02- 05ER15666

## References

1. B. J. Xu, Y. Bhawe and M. E. Davis, *Chem. Mater.*, 2013, **25**, 1564-1571.
2. W. F. Zhang, F. Liu, Q. Q. Li, Q. L. Shou, J. P. Cheng, L. Zhang, B. J. Nelson and X. B. Zhang, *Phys. Chem. Chem. Phys.*, 2012, **14**, 16331-16337.
3. S. C. Abrahams and B. A. Calhoun, *Acta Crystallogr.*, 1953, **6**, 105-106.
4. J. D. Dunitz and L. E. Orgel, *J. Phys. Chem. Solids*, 1957, **3**, 318-323.
5. D. S. McClure, *Phys. Chem. Solids*, 1957, **3**, 311-317.
6. A. H. Eschenfelder, *J. Appl. Phys.*, 1958, **29**, 378-380.
7. S. K. Sahu, R. Ganesan and T. Gnanasekaran, *J. Nucl. Mater.*, 2008, **376**, 366-370.
8. S. K. Sahu, R. Ganesan and T. Gnanasekaran, *J. Chem. Thermodyn.*, 2010, **42**, 1-7.
9. S. K. Sahu, R. Ganesan and T. Gnanasekaran, *J. Nucl. Mater.*, 2012, **426**, 214-222.
10. S. K. Sahu, R. Ganesan and T. Gnanasekaran, *J. Chem. Thermodyn.*, 2013, **56**, 57-59.
11. K. Schwerdt and A. Muan, *Trans. Metall. Soc. Aime*, 1967, **239**, 1114
12. R. Subramanian, R. Dieckmann, G. Eriksson and A. Pelton, *J. Phys. Chem. Solids*, 1994, **55**, 391-404.
13. M. Takahashi, J. R. Guimarae and M. E. Fine, *J. Am. Ceram. Soc.*, 1971, **54**, 291-295.
14. S. K. Sahu, D. K. Unruh, T. Z. Forbes and A. Navrotsky, *Chem. Mater.*, 2014, **26**, 5105-5112.
15. H. J. Vanhook and M. L. Keith, *Am. Miner.*, 1958, **43**, 69-83.
16. D. G. Wickham, *J. Inorg. Nucl. Chem.*, 1969, **31**, 313
17. I. V. Gordeev, Y. D. Tretyakov and K. G. Khomyakov, *Zh. Neorg. Khim.*, 1964, **9**, 164-168.
18. S. K. Sahu and A. Navrotsky, High-Temperature Materials Chemistry and Thermodynamics, in High Temperature Materials and Mechanisms, CRC Press, 2014, pp. 17-38.
19. S. Zlotnik, S. K. Sahu, A. Navrotsky and P. M. Vilarinho, *Chem. - Eur. J.*, 2015, **21**, 5231-5237.
20. S. K. Sahu, M. Sahu, R. S. Srinivasa and T. Gnanasekaran, *Monatsh. Chem.*, 2012, **143**, 1207-1214.
21. A. Navrotsky, *J. Inorg. Nucl. Chem.*, 1969, **31**, 59-72.
22. S. Fritsch and A. Navrotsky, *J. Am. Ceram. Soc.*, 1996, **79**, 1761-1768.
23. N. Tiberg and A. Muan, *Metall. Trans.*, 1970, **1**, 435-439.
24. C. Landolt and A. Muan, *J. Inorg. Nucl. Chem.*, 1969, **31**, 1319-1326.
25. E. Aukrust and A. Muan, *Trans. Metall. Soc. Aime*, 1964, **230**, 1395-1399.
26. E. Aukrust and A. Muan, *Jom-Journal of Metals*, 1964, **16**, 110
27. E. Aukrust and A. Muan, *Trans. Metall. Soc. Aime*, 1964, **230**, 378-382.
28. H. Schmalzr and J. D. Tretjako, *Ber. Bunsen-Ges. Phys. Chem.*, 1966, **70**, 180-189.
29. G. H. Jonker, *J. Phys. Chem. Solids*, 1959, **9**, 165-175.
30. W. Müller and H. Schmalzried, *Ber. Bunsen-Ges. Phys. Chem.*, 1964, **68**, 270-276.
31. S. Guillemet-Fritsch, A. Navrotsky, P. Tailhades, H. Coradin and M. Wang, *J. Solid State Chem.*, 2005, **178**, 106-113.
32. A. Navrotsky, C. C. Ma, K. Lilova and N. Birkner, *Science*, 2010, **330**, 199-201.
33. H. S. C. O'Neill and A. Navrotsky, *Am. Mineral.*, 1984, **69**, 733-753.
34. R. T. Olsson, G. Salazar-Alvarez, M. S. Hedenqvist, U. W. Gedde, F. Lindberg and S. J. Savage, *Chem. Mater.*, 2005, **17**, 5109-5118.

35. T. A. S. Ferreira, J. C. Waerenborgh, M. H. R. M. Mendonca, M. R. Nunes and F. M. Costa, *Solid State Sci.*, 2003, **5**, 383-392.
36. G. V. M. Jacintho, A. G. Brolo, P. Corio, P. A. Z. Suarez and J. C. Rubim, *J. Phys. Chem. C*, 2009, **113**, 7684-7691.
37. S. J. Smith, B. Huang, S. Liu, Q. Liu, R. E. Olsen, J. Boerio-Goates and B. F. Woodfield, *Nanoscale*, 2015, **7**, 144-156.
38. S. Brunauer, P. H. Emmett and E. Teller, *J. Amer. Chem. Soc.*, 1938, **60**, 309-319.
39. A. Navrotsky, *Phys. Chem. Miner.*, 1977, **2**, 89-104.
40. A. Navrotsky, *Phys. Chem. Miner.*, 1997, **24**, 222-241.
41. S. K. Sahu, P. S. Maram and A. Navrotsky, *J. Am. Ceram. Soc.*, 2013, **96**, 3670-3676.
42. B. D. Cullity, *Elements of X-Ray Diffraction*, Addison-Wesley Pub. Co., 1956.
43. K. I. Lilova, F. Xu, K. M. Rosso, C. I. Pearce, S. Kamali and A. Navrotsky, *Am. Mineral.*, 2012, **97**, 164-175.
44. G. C. C. Costa, S. V. Ushakov, R. H. R. Castro, A. Navrotsky and R. Muccillo, *Chem. Mater.*, 2010, **22**, 2937-2945.
45. T. J. Park, A. A. Levchenko, H. J. Zhou, S. S. Wong and A. Navrotsky, *J. Mater. Chem.*, 2010, **20**, 8639-8645.
46. P. Zhang, F. Xu, A. Navrotsky, J. S. Lee, S. T. Kim and J. Liu, *Chem. Mater.*, 2007, **19**, 5687-5693.
47. A. A. Levchenko, G. S. Li, J. Boerio-Goates, B. F. Woodfield and A. Navrotsky, *Chem. Mater.*, 2006, **18**, 6324-6332.
48. R. A. Robie, B. S. Hemingway and J. R. Fisher, *Thermodynamic Properties of Minerals and Related Substances at 298.15 K and 1 Bar (10<sup>5</sup> Pascals) Pressure and at Higher Temperatures*, Government Printing Office, 1978.
49. K. I. Lilova, C. I. Pearce, K. M. Rosso and A. Navrotsky, *Chem.phys.chem.*, 2014, **15**, 3655-3622.
50. A. Navrotsky, *Am. Mineral.*, 1986, **71**, 1160-1169.
51. H. S. C. O'Neill and A. Navrotsky, *Am. Mineral.*, 1983, **68**, 181-194.
52. V. A. M. Brabers and P. Dekker, *Phys. Status Solidi*, 1968, **29**, 73-76
53. A. Navrotsky and O. J. Kleppa, *J. Inorg. Nucl. Chem.*, 1967, **29**, 2701-2714.

## Table captions

**Table 1:** BET surface area, drop solution enthalpies and surface energy of  $(1-x)\text{Fe}_3\text{O}_4 - x\text{M}_3\text{O}_4$  (M: Fe, Co) spinel solid solutions

**Table 2:** Thermochemical cycle used for water correction for energy of hydrous surface

**Table 3:** Thermochemical cycle to calculate the enthalpies of mixing of  $(1-x)\text{Fe}_3\text{O}_4 - x\text{Mn}_3\text{O}_4$  spinel solution relative to c- $\text{Mn}_3\text{O}_4$  and c- $\text{Fe}_3\text{O}_4$

**Table 4:** Calculated enthalpies of mixing (kJ/mol) for  $(1-x)\text{Fe}_3\text{O}_4 - x\text{M}_3\text{O}_4$  solid solutions using O'Neill and Navrotsky model

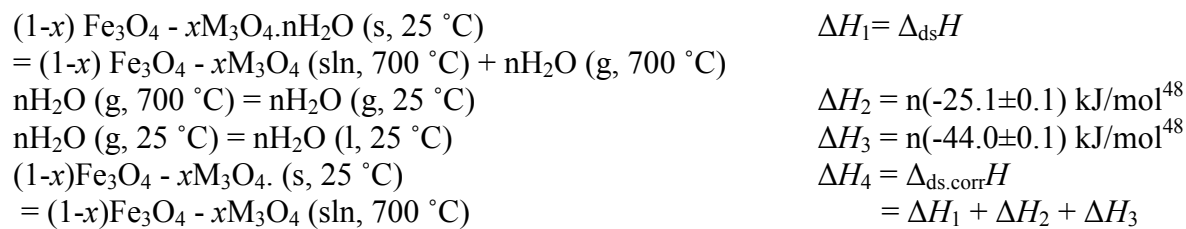
**Table 5:** Cation distributions, configurational entropy and entropies of mixing in  $(1-x)\text{Fe}_3\text{O}_4 - x\text{M}_3\text{O}_4$  (M: Co, Mn) spinel solid solutions (keeping  $\text{M}^{3+}$  in octahedral site and random distribution of the remaining ions)

**Table 6:** Calculation of entropies of mixing in  $(1-x)\text{Fe}_3\text{O}_4 - x\text{Co}_3\text{O}_4$  solid solutions

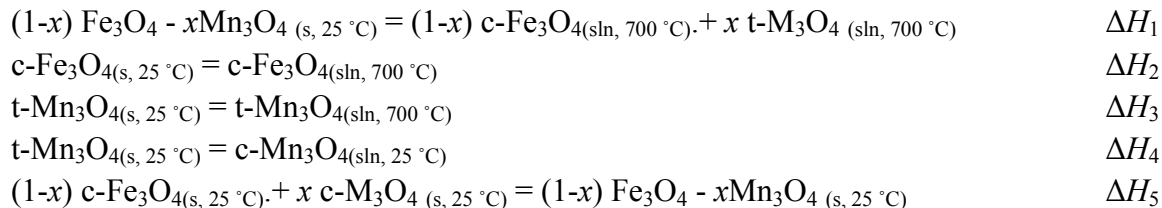
**Table 7:** Calculation of entropies of mixing in  $(1-x)\text{Fe}_3\text{O}_4 - x\text{Mn}_3\text{O}_4$  solid solutions

**Table -1:** BET surface area, drop solution enthalpies and surface energy of  $(1-x)\text{Fe}_3\text{O}_4 - x\text{M}_3\text{O}_4$  (M: Fe, Co) spinel solid solutions

| Compositions                                  | XRD particle size (nm)                     | Surface area          |                              |                              | $(\Delta_{\text{ds}}H)$ , kJ/mol |                   | Surface Energy, $\text{J/m}^2$ |                 |
|-----------------------------------------------|--------------------------------------------|-----------------------|------------------------------|------------------------------|----------------------------------|-------------------|--------------------------------|-----------------|
|                                               |                                            | $\text{m}^2/\text{g}$ | Nano $\text{m}^2/\text{mol}$ | Bulk $\text{m}^2/\text{mol}$ | Nano                             | Bulk              |                                |                 |
| $\text{Fe}_3\text{O}_4\text{-Co}_3\text{O}_4$ | $\text{Fe}_3\text{O}_4$                    |                       |                              | $0 \pm 0.9$                  | $0.3 \pm 1.0$                    | $15.2 \pm 1.0$    | $0.8^{43}$                     |                 |
|                                               | $\text{Co}_{0.6}\text{Fe}_{2.4}\text{O}_4$ | $12.8 \pm 1.8$        | $98.6 \pm 1.1$               | $22945.3 \pm 256.0$          | $2.3 \pm 2.3$                    | $84.6 \pm 3.5$    | $100.9 \pm 2.3$                | $0.71 \pm 0.12$ |
|                                               | $\text{CoFe}_2\text{O}_4$                  | $19.5 \pm 3.6$        | $54.8 \pm 0.2$               | $12859.6 \pm 46.9$           | $0.9 \pm 2.7$                    | $121.6 \pm 2.7$   | $132.3 \pm 2.1$                | $0.83 \pm 0.24$ |
|                                               | $\text{Co}_{1.5}\text{Fe}_{1.5}\text{O}_4$ | $17.8 \pm 1.9$        | $51.3 \pm 0.3$               | $12092.3 \pm 70.7$           | $1.9 \pm 3.6$                    | $142.2 \pm 2.4$   | $149.7 \pm 2.4$                | $0.62 \pm 0.26$ |
|                                               | $\text{Co}_2\text{FeO}_4$                  | $12.6 \pm 2.4$        | $86.5 \pm 0.6$               | $20569.0 \pm 142.6$          | $0.0 \pm 2.2$                    | $167.4 \pm 2.2$   | $182.5.5 \pm 2.0$              | $0.73 \pm 0.13$ |
|                                               | $\text{Co}_{2.4}\text{Fe}_{0.6}\text{O}_4$ | $13.4 \pm 1.3$        | $73.1 \pm 0.5$               | $17454.9 \pm 119.4$          | $1.4 \pm 3.9$                    | $183.8 \pm 3.5$   | $195.4 \pm 3.4$                | $0.67 \pm 0.20$ |
|                                               | $\text{Co}_3\text{O}_4$                    | $16.8 \pm 2.2$        | $43.8 \pm 0.6$               | $10544.5 \pm 144.5$          | $481.6 \pm 8.5$                  | $225.0 \pm 4.4$   | $232.21 \pm 2.1$               | $0.72 \pm 0.46$ |
| $\text{Fe}_3\text{O}_4\text{-Mn}_3\text{O}_4$ | $\text{Fe}_3\text{O}_4$                    |                       |                              | $0 \pm 0.9$                  | $0.3 \pm 1.0$                    | $15.2 \pm 1.0$    | $0.8^{43}$                     |                 |
|                                               | $\text{MnFe}_2\text{O}_4$                  | $21.2 \pm 2.5$        | $62.7 \pm 0.6$               | $14469.5 \pm 138.4$          | $1.8 \pm 3.3$                    | $89.54 \pm 3.64$  | $99.3 \pm 2.1$                 | $0.67 \pm 0.24$ |
|                                               | $\text{Mn}_{1.5}\text{Fe}_{1.5}\text{O}_4$ | $20.9 \pm 2.3$        | $62.4 \pm 0.4$               | $14437.3 \pm 92.1$           | $0.0 \pm 1.7$                    | $99.97 \pm 3.58$  | $110.5 \pm 2.4$                | $0.73 \pm 0.27$ |
|                                               | $\text{Mn}_2\text{FeO}_4$                  | $17.6 \pm 1.8$        | $80.5 \pm 0.4$               | $18485.5 \pm 91.9$           | $1.4 \pm 3.1$                    | $113.78 \pm 2.99$ | $129.5 \pm 2.0$                | $0.85 \pm 0.23$ |
|                                               | $\text{Mn}_{2.4}\text{Fe}_{0.6}\text{O}_4$ | $19.7 \pm 2.1$        | $66.3 \pm 0.1$               | $15215.5 \pm 22.9$           | $457.6 \pm 5.2$                  | $128.71 \pm 4.51$ | $142.1 \pm 3.4$                | $0.88 \pm 0.44$ |
|                                               | $\text{Mn}_3\text{O}_4$                    | $23.1 \pm 2.7$        | $40.9 \pm 0.1$               | $9349.3 \pm 91.5$            | $0.9 \pm 1.8$                    | $163.14 \pm 2.19$ | $170.6 \pm 2.1$                | $0.84 \pm 0.29$ |

**Table 2:** Thermochemical cycle used for water correction for energy of hydrous surface

**Table -3:** Thermochemical cycle to calculate the enthalpies of mixing of  $(1-x)\text{Fe}_3\text{O}_4 - x\text{Mn}_3\text{O}_4$  spinel solution relative to c- $\text{Mn}_3\text{O}_4$  and c- $\text{Fe}_3\text{O}_4$



Where

$\Delta H_1$  = Drop solution enthalpies of  $(1-x) \text{Fe}_3\text{O}_4 - x\text{Mn}_3\text{O}_4$  solid solutions for  $0.6 \leq x_{\text{Mn}_3\text{O}_4} \leq 1$   $3\text{Na}_2\text{O} \cdot 4\text{MoO}_3$  solvent at  $700^\circ\text{C}$  under flowing oxygen gas

$\Delta H_2$  = Drop solution enthalpies of  $\text{Fe}_3\text{O}_4$  in  $3\text{Na}_2\text{O} \cdot 4\text{MoO}_3$  solvent at  $700^\circ\text{C}$  under flowing oxygen gas

$\Delta H_3$  = Drop solution enthalpies of t- $\text{Mn}_3\text{O}_4$  in  $3\text{Na}_2\text{O} \cdot 4\text{MoO}_3$  solvent at  $700^\circ\text{C}$  under flowing oxygen gas

$\Delta H_4$  = tetragonal to cubic phase transition enthalpy of  $\Delta_{\text{ds,corr}}H$  of  $\text{Mn}_3\text{O}_4$

$\Delta H_5 = -\Delta H_1 + (1-x) \Delta H_2 + x \Delta H_3 - x \Delta H_4$  = Enthalpy of mixing/formation of cubic  $(1-x) \text{Fe}_3\text{O}_4 - x\text{Mn}_3\text{O}_4$  solid solutions from c- $\text{Fe}_3\text{O}_4$  and c- $\text{Mn}_3\text{O}_4$

**Table-4:** Calculated Enthalpies of mixing (kJ/mol) for  $(1-x)\text{Fe}_3\text{O}_4-x\text{M}_3\text{O}_4$  solid solutions by Navrotsky model

| Compositions                              | $x_{\text{M}_3\text{O}_4}$ | Enthalpies of mixing (kJ/mol) for $(1-x)\text{Fe}_3\text{O}_4 - x\text{Co}_3\text{O}_4$ solid solutions |                            |                            | Enthalpies of mixing (kJ/mol) for $(1-x)\text{Fe}_3\text{O}_4 - x\text{Mn}_3\text{O}_4$ solid solutions |                            |                                                                  |                                                                  |
|-------------------------------------------|----------------------------|---------------------------------------------------------------------------------------------------------|----------------------------|----------------------------|---------------------------------------------------------------------------------------------------------|----------------------------|------------------------------------------------------------------|------------------------------------------------------------------|
|                                           |                            | $\Delta_{\text{ox/red}}H$<br>(mix)                                                                      | $\Delta_{\text{mix,c,d}}H$ | $\Delta_{\text{mix,s,m}}H$ | $\Delta_{\text{ox/red}}H$<br>(mix)                                                                      | $\Delta_{\text{mix,c,d}}H$ | $\Delta_{\text{mix,s,m}}H$<br>(with t- $\text{Mn}_3\text{O}_4$ ) | $\Delta_{\text{mix,s,m}}H$<br>(with c- $\text{Mn}_3\text{O}_4$ ) |
| $\text{Fe}_3\text{O}_4$                   | 0                          | 0                                                                                                       | 0                          | 0                          | 0                                                                                                       | 0                          | 0.0                                                              | 0                                                                |
| $\text{M}_{0.3}\text{Fe}_{2.7}\text{O}_4$ | 0.1                        | -14.6                                                                                                   | -0.4                       | 0.1                        | -11.5                                                                                                   | -0.2                       | 0.4                                                              | 0.3                                                              |
| $\text{M}_{0.6}\text{Fe}_{2.4}\text{O}_4$ | 0.2                        | -28.8                                                                                                   | -1.9                       | 0.6                        | -22.9                                                                                                   | -0.5                       | 0.8                                                              | 0.8                                                              |
| $\text{M}_{0.9}\text{Fe}_{2.1}\text{O}_4$ | 0.3                        | -42.5                                                                                                   | -4.9                       | 1.4                        | -34.2                                                                                                   | -1.0                       | 1.1                                                              | 1.1                                                              |
| $\text{MFe}_2\text{O}_4$                  | 0.33                       | -47.3                                                                                                   | -6.3                       | 1.6                        | -38.2                                                                                                   | -1.2                       | 1.1                                                              | 1.1                                                              |
| $\text{M}_{1.2}\text{Fe}_{1.8}\text{O}_4$ | 0.4                        | -42.0                                                                                                   | -6.4                       | 2.1                        | -34.1                                                                                                   | -1.9                       | 1.0                                                              | 1.0                                                              |
| $\text{M}_{1.5}\text{Fe}_{1.5}\text{O}_4$ | 0.5                        | -34.5                                                                                                   | -9.9                       | 2.5                        | -28.3                                                                                                   | -2.1                       | 0.9                                                              | 0.9                                                              |
| $\text{M}_{1.8}\text{Fe}_{1.2}\text{O}_4$ | 0.6                        | -27.2                                                                                                   | -5.3                       | 2.4                        | -22.6                                                                                                   | -5.8                       | 14.3                                                             | 0.8                                                              |
| $\text{M}_2\text{FeO}_4$                  | 0.67                       | -22.2                                                                                                   | -8.5                       | 2.0                        | -18.6                                                                                                   | -5.1                       | 17.0                                                             | 0.9                                                              |
| $\text{M}_{2.1}\text{Fe}_{0.9}\text{O}_4$ | 0.7                        | -20.1                                                                                                   | -3.8                       | 1.7                        | -16.9                                                                                                   | -7.6                       | 16.6                                                             | 1.0                                                              |
| $\text{M}_{2.4}\text{Fe}_{0.6}\text{O}_4$ | 0.8                        | -13.2                                                                                                   | -1.9                       | 0.8                        | -11.2                                                                                                   | -6.4                       | 11.3                                                             | 1.4                                                              |
| $\text{M}_{2.7}\text{Fe}_{0.3}\text{O}_4$ | 0.9                        | -6.5                                                                                                    | -0.8                       | 0.2                        | -5.6                                                                                                    | -4.0                       | 3.7                                                              | 1.4                                                              |
| $\text{M}_3\text{O}_4$                    | 1                          | 0                                                                                                       | 0                          | 0                          | 0                                                                                                       | 0                          | 0                                                                | 0                                                                |

**Table 5:** Cation distributions, configurational entropy and entropies of mixing in  $(1-x)\text{Fe}_3\text{O}_4 - x\text{M}_3\text{O}_4$  (M: Co, Mn) spinel solid solutions (keeping  $\text{M}^{3+}$  in octahedral site and random distribution of the remaining ions)

| Compositions                              | $x_{\text{M}_3\text{O}_4}$ | Cation distributions                                                                                                                     | $S_{\text{conf}}$ | $\Delta_{\text{mix}}S$ , J/(mol K) |
|-------------------------------------------|----------------------------|------------------------------------------------------------------------------------------------------------------------------------------|-------------------|------------------------------------|
| $\text{Fe}_3\text{O}_4$                   | 0                          | $\text{Fe}^{3+}[\text{Fe}^{2+}\text{Fe}^{3+}]\text{O}_4$                                                                                 | 11.53             | 0.00                               |
| $\text{M}_{0.3}\text{Fe}_{2.7}\text{O}_4$ | 0.1                        | $\text{M}_{0.1}^{2+}\text{Fe}_{0.7/3}^{2+}\text{Fe}_{2/3}^{3+}[\text{Fe}_{1.4/3}^{2+}\text{M}_{0.2}^{2+}\text{Fe}_{4/3}^{3+}]\text{O}_4$ | 20.95             | 10.58                              |
| $\text{M}_{0.6}\text{Fe}_{2.4}\text{O}_4$ | 0.2                        | $\text{M}_{0.2}^{2+}\text{Fe}_{0.4/3}^{2+}\text{Fe}_{2/3}^{3+}[\text{Fe}_{0.8/3}^{2+}\text{M}_{0.4}^{2+}\text{Fe}_{4/3}^{3+}]\text{O}_4$ | 21.47             | 12.25                              |
| $\text{M}_{0.9}\text{Fe}_{2.1}\text{O}_4$ | 0.3                        | $\text{M}_{0.3}^{2+}\text{Fe}_{0.1/3}^{2+}\text{Fe}_{2/3}^{3+}[\text{Fe}_{0.2/3}^{2+}\text{M}_{0.6}^{2+}\text{Fe}_{4/3}^{3+}]\text{O}_4$ | 18.58             | 10.51                              |
| $\text{MFe}_2\text{O}_4$                  | 0.33                       | $\text{M}_{1/3}^{2+}\text{Fe}_{2/3}^{3+}[\text{M}_{2/3}^{2+}\text{Fe}_{4/3}^{3+}]\text{O}_4$                                             | 15.88             | 8.15                               |
| $\text{M}_{1.2}\text{Fe}_{1.8}\text{O}_4$ | 0.4                        | $\text{M}_{0.4}^{2+}\text{Fe}_{0.6}^{3+}[\text{M}_{0.6}^{2+}\text{Fe}_{1.2}^{3+}\text{M}_{0.2}^{3+}]\text{O}_4$                          | 20.53             | 13.61                              |
| $\text{M}_{1.5}\text{Fe}_{1.5}\text{O}_4$ | 0.5                        | $\text{M}_{1/3}^{2+}\text{Fe}_{2/3}^{3+}[\text{M}_{2/3}^{2+}\text{Fe}_{5/6}^{3+}\text{M}_{1/2}^{3+}]\text{O}_4$                          | 23.21             | 17.45                              |
| $\text{M}_{1.8}\text{Fe}_{1.2}\text{O}_4$ | 0.6                        | $\text{M}_{0.6}^{2+}\text{Fe}_{0.4}^{3+}[\text{M}_{0.4}^{2+}\text{Fe}_{0.8}^{3+}\text{M}_{0.8}^{3+}]\text{O}_4$                          | 23.14             | 18.53                              |
| $\text{M}_2\text{FeO}_4$                  | 0.67                       | $\text{M}_{0.5}^{2+}\text{Fe}_{0.5}^{3+}[\text{M}_{0.5}^{2+}\text{Fe}_{0.5}^{3+}\text{M}^{3+}]\text{O}_4$                                | 23.05             | 19.25                              |
| $\text{M}_{2.1}\text{Fe}_{0.9}\text{O}_4$ | 0.7                        | $\text{M}_{0.7}^{2+}\text{Fe}_{0.3}^{3+}[\text{M}_{0.3}^{2+}\text{Fe}_{0.6}^{3+}\text{M}_{1.1}^{3+}]\text{O}_4$                          | 21.28             | 17.83                              |
| $\text{M}_{2.4}\text{Fe}_{0.6}\text{O}_4$ | 0.8                        | $\text{M}_{0.8}^{2+}\text{Fe}_{0.2}^{3+}[\text{M}_{0.2}^{2+}\text{Fe}_{0.4}^{3+}\text{M}_{1.4}^{3+}]\text{O}_4$                          | 17.49             | 15.19                              |
| $\text{M}_{2.7}\text{Fe}_{0.3}\text{O}_4$ | 0.9                        | $\text{M}_{0.9}^{2+}\text{Fe}_{0.1}^{3+}[\text{M}_{0.1}^{2+}\text{Fe}_{0.3}^{3+}\text{M}_{1.7}^{3+}]\text{O}_4$                          | 12.22             | 11.07                              |
| $\text{M}_3\text{O}_4$                    | 1                          | $\text{M}^{2+}[\text{M}_2^{3+}]\text{O}_4$                                                                                               | 0.00              | 0.00                               |

**Table -6:** Calculation of entropies of mixing in  $(1-x)\text{Fe}_3\text{O}_4 - x\text{Co}_3\text{O}_4$  solid solutions

| $x_{\text{Co}_3\text{O}_4}$ | $\Delta_{\text{mix}}G$ (kJ/mol) | $\Delta_{\text{mix}}H$ (kJ/mol) | $\Delta_{\text{mix}}S$ , J/(K mol) |       |
|-----------------------------|---------------------------------|---------------------------------|------------------------------------|-------|
|                             | A                               | B                               | C                                  | D     |
| 0.1                         | -20.51                          | -20.30                          | 0.14                               | 10.58 |
| 0.2                         | -39.76                          | -40.79                          | -0.70                              | 12.25 |
| 0.3                         | -54.41                          | -44.80                          | 6.52                               | 10.51 |
| 0.4                         | -58.59                          | -39.07                          | 13.25                              | 13.61 |
| 0.5                         | -54.41                          | -27.77                          | 18.08                              | 17.45 |
| 0.6                         | -45.20                          | -22.60                          | 15.34                              | 19.25 |
| 0.7                         | -37.67                          | -15.52                          | 15.03                              | 17.83 |
| 0.8                         | -29.30                          | -5.02                           | 16.48                              | 15.19 |
| 0.9                         | -16.74                          | -1.02                           | 10.67                              | 11.07 |

- (A)  $\Delta_{\text{mix}}G$  (formation from cubic end members) calculated from activity data Aukrust and Muan<sup>26</sup> at 1200 °C
- (B)  $\Delta_{\text{mix}}H$  calculated from the present work
- (C) Experimentally determined entropy of mixing,  $\Delta_{\text{mix}}S = (\Delta_{\text{mix}}H - \Delta_{\text{mix}}G)/T$
- (D) Configurational entropies of mixing. ( $\text{Co}_3\text{O}_4$  normal,  $\text{Fe}_3\text{O}_4$  inverse and cation distributions:  $\text{Co}^{3+}$  in octahedral sites and random distribution of the remaining ions)

**Table -7:** Calculation of entropies of mixing in  $(1-x)\text{Fe}_3\text{O}_4-x\text{Mn}_3\text{O}_4$  solid solutions

| $x_{\text{Mn}_3\text{O}_4}$ | $\Delta_{\text{mix}}G$ (kJ/mol) | $\Delta_{\text{mix}}H$ (kJ/mol) | $\Delta_{\text{mix}}S$ , J/(K mol) |          |
|-----------------------------|---------------------------------|---------------------------------|------------------------------------|----------|
|                             | <b>A</b>                        | <b>B</b>                        | <b>C</b>                           | <b>D</b> |
| 0.1                         | -14.60                          | -9.26                           | 4.19                               | 10.58    |
| 0.2                         | -21.70                          | -20.97                          | 0.57                               | 12.25    |
| 0.3                         | -29.30                          | -30.38                          | -0.85                              | 10.51    |
| 0.4                         | -37.20                          | -27.01                          | 8.00                               | 13.61    |
| 0.5                         | -41.00                          | -20.17                          | 16.36                              | 17.45    |
| 0.6                         | -46.00                          | -18.49                          | 21.61                              | 19.25    |
| 0.7                         | -46.90                          | -16.71                          | 23.72                              | 17.83    |
| 0.8                         | -37.70                          | -10.85                          | 21.09                              | 15.19    |
| 0.9                         | -25.10                          | -5.50                           | 15.40                              | 11.07    |

(A)  $\Delta_{\text{mix}}G$  (formation from cubic end members) calculated from activity data of Tret'yakov<sup>17</sup> at 1000 °C

(B)  $\Delta_{\text{mix}}H$  calculated from the present work

(C) Experimentally determined entropy of mixing,  $\Delta_{\text{mix}}S = (\Delta_{\text{mix}}H - \Delta_{\text{mix}}G)/T$

(D) Configurational entropies of mixing. ( $\text{Mn}_3\text{O}_4$  normal,  $\text{Fe}_3\text{O}_4$  inverse and cation distributions:  $\text{Mn}^{3+}$  in octahedral site and random distribution of the remaining ions)

**Figure captions**

**Figure 1:** Drop solution enthalpies ( $\Delta_{ds}H$ ) of  $(1-x)\text{Fe}_3\text{O}_4 - x\text{Co}_3\text{O}_4$  solid solutions in molten  $3\text{Na}_2\text{O} \cdot 4\text{MoO}_3$  at  $700\text{ }^\circ\text{C}$ . The curve represents a third degree polynomial fit of the experimental data:  $y = A+B_1x+B_2x^2+B_3x^3$ .

**Figure 2:** Drop solution enthalpies ( $\Delta_{ds}H$ ) of  $(1-x)\text{Fe}_3\text{O}_4 - x\text{Mn}_3\text{O}_4$  solid solutions in  $3\text{Na}_2\text{O} \cdot 4\text{MoO}_3$  at  $700\text{ }^\circ\text{C}$ . The curve represents a third degree polynomial fit of the experimental data:  $y = A+B_1x+B_2x^2+B_3x^3$ .

**Figure 3:** Enthalpy of mixing ( $\Delta_{mix}H$ ) of  $(1-x)\text{Fe}_3\text{O}_4 - x\text{Co}_3\text{O}_4$  solid solutions. The curved line represents the  $\Delta_{mix}H$  calculated employing the O'Neill and Navrotsky thermodynamic model<sup>33</sup>.

**Figure 4(a):** Enthalpy of mixing ( $\Delta_{mix}H$ ) of  $(1-x)\text{Fe}_3\text{O}_4 - x\text{Mn}_3\text{O}_4$  solid solutions with cubic  $\text{Fe}_3\text{O}_4$  and tetragonal  $\text{Mn}_3\text{O}_4$  end members. The curved line represents the  $\Delta_{mix}H$  calculated employing the O'Neill and Navrotsky thermodynamic model<sup>33</sup>.

**Figure 4(b):** Enthalpy of mixing ( $\Delta_{mix}H$ ) of  $(1-x)\text{Fe}_3\text{O}_4 - x\text{Mn}_3\text{O}_4$  solid solutions with cubic  $\text{Fe}_3\text{O}_4$  and cubic  $\text{Mn}_3\text{O}_4$  end members. The curved line represents the  $\Delta_{mix}H$  calculated employing the O'Neill and Navrotsky thermodynamic model<sup>33</sup>.

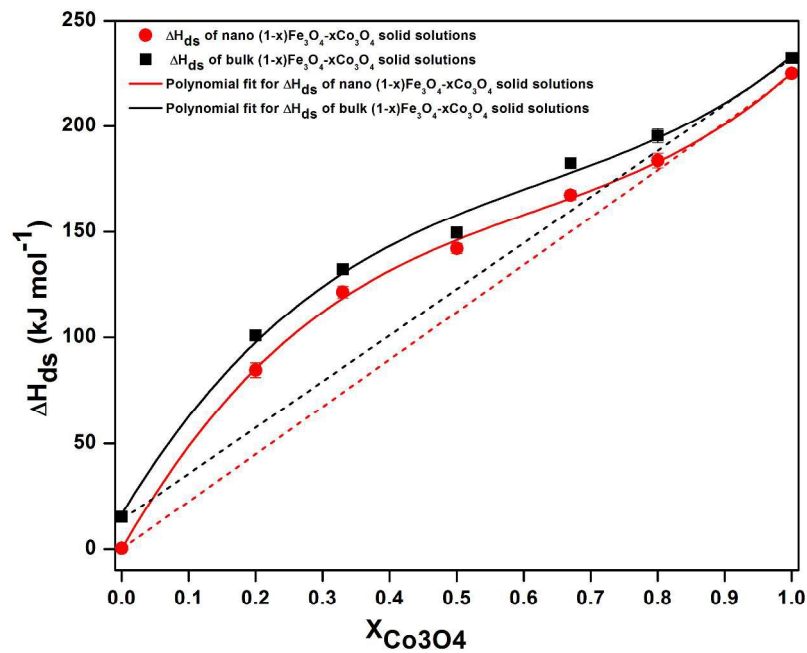
**Figure 5(a):** Configurational entropy ( $S_{\text{Conf}}$ ) in  $(1-x)\text{Fe}_3\text{O}_4 - x\text{M}_3\text{O}_4$  ( $M = \text{Co}, \text{Mn}$ ) solid solutions. Site occupancies are calculated using the O'Neill and Navrotsky model<sup>33</sup>. (b): Entropies of mixing ( $\Delta_{mix}S$ ) in  $(1-x)\text{Fe}_3\text{O}_4 - x\text{M}_3\text{O}_4$  solid solutions.

**Figure 5(b):** Entropies of mixing ( $\Delta_{mix}S$ ) in  $(1-x)\text{Fe}_3\text{O}_4 - x\text{M}_3\text{O}_4$  solid solutions.

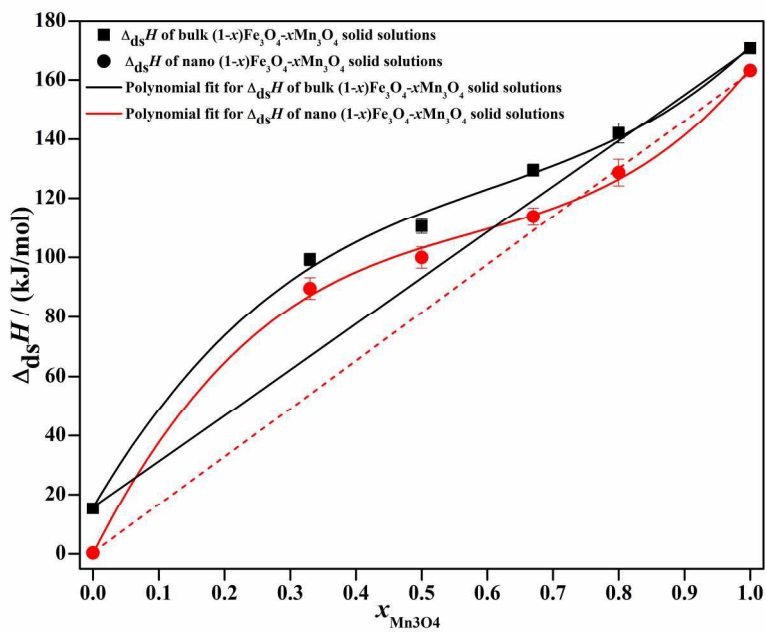
**Figure 6(a):** Gibbs free energy of mixing ( $\Delta_{mix}G$ ) of  $(1-x)\text{Fe}_3\text{O}_4 - x\text{Co}_3\text{O}_4$  solid solutions at  $1200\text{ }^\circ\text{C}$ .

**Figure 6(b):** Gibbs free energy of mixing ( $\Delta_{mix}G$ ) of  $(1-x)\text{Fe}_3\text{O}_4 - x\text{Mn}_3\text{O}_4$  solid solutions at  $1000\text{ }^\circ\text{C}$ , with cubic  $\text{Fe}_3\text{O}_4$  and tetragonal  $\text{Mn}_3\text{O}_4$  end members.

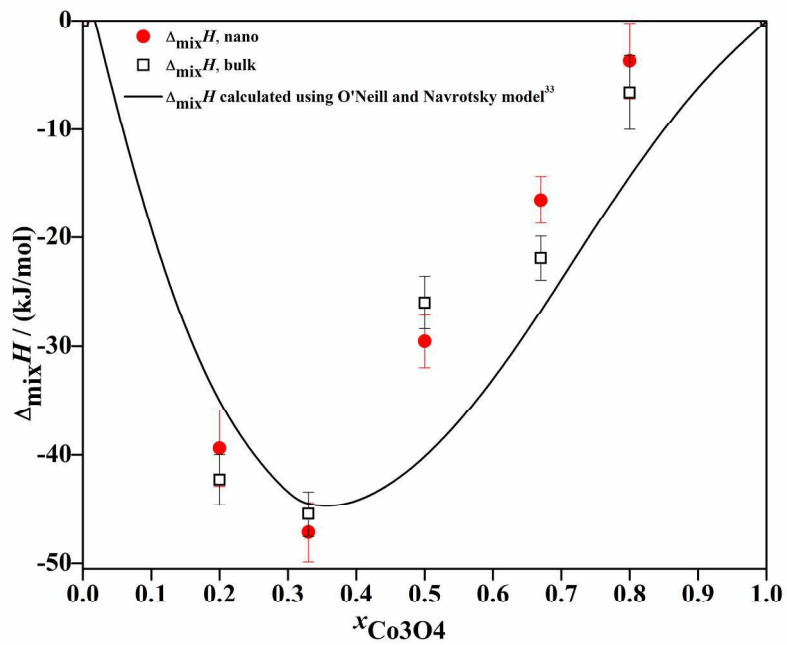
**Figure 6(c):** Gibbs energy of mixing ( $\Delta_{mix}G$ ) of  $(1-x)\text{Fe}_3\text{O}_4 - x\text{Mn}_3\text{O}_4$  solid solutions at  $1000\text{ }^\circ\text{C}$  with cubic  $\text{Fe}_3\text{O}_4$  and cubic  $\text{Mn}_3\text{O}_4$  end members.



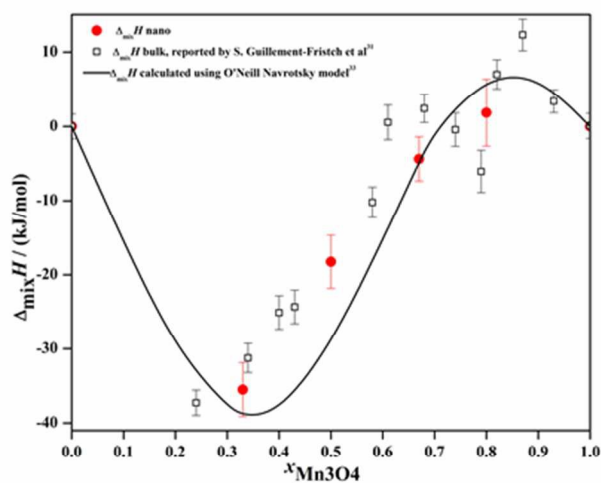
271x207mm (300 x 300 DPI)



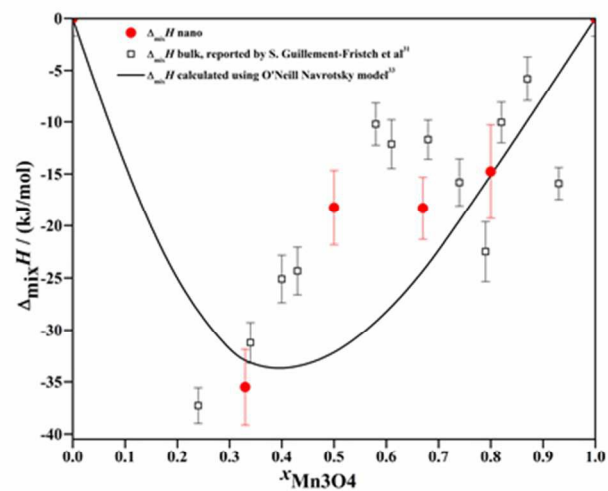
207x158mm (300 x 300 DPI)



207x158mm (300 x 300 DPI)

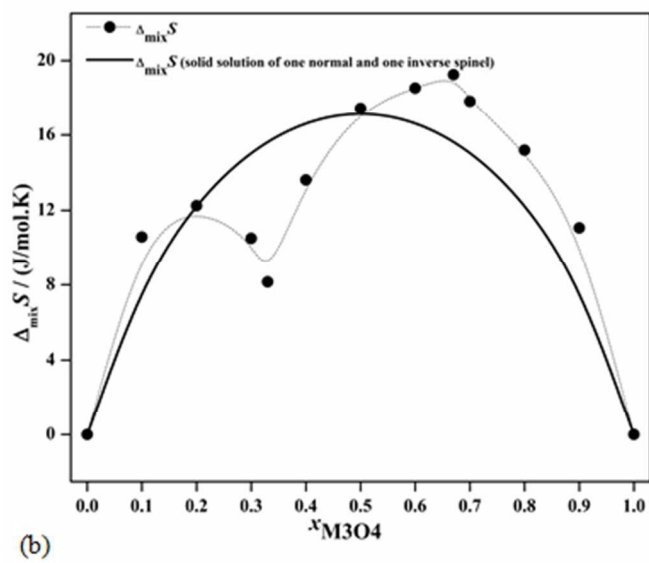
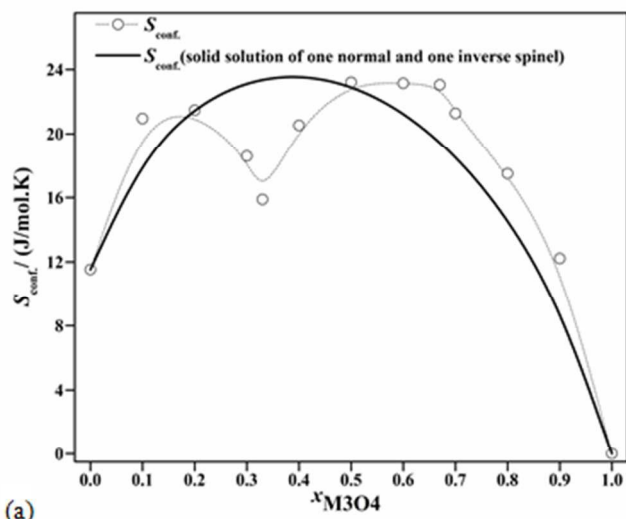


(a)

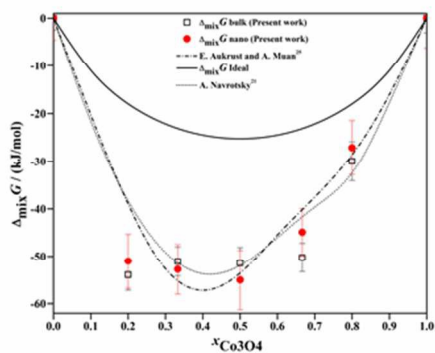


(b)

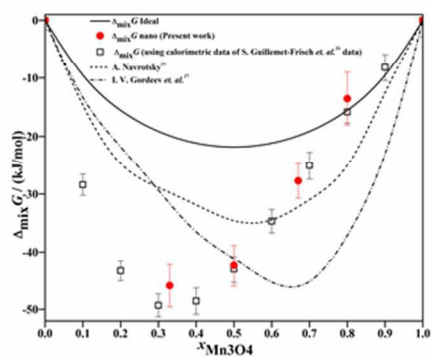
144x213mm (96 x 96 DPI)



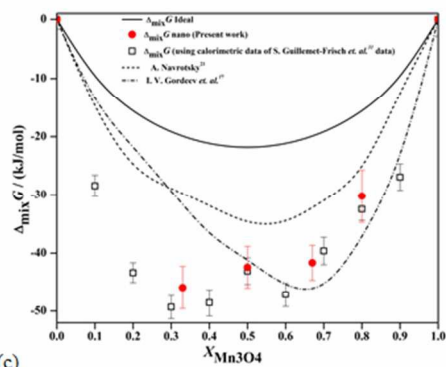
101x186mm (96 x 96 DPI)



(a)



(b)



(c)

201x177mm (96 x 96 DPI)